# Structural Design Optimization for CFRP in a Personal Aerial Vehicle Propulsor Boom

**A. Hardman[a], L. Crispo[a], T. Sirola[a], S. Jalayer[a], J. Ann[b], J. Lee[b], J. H. Song[c], I. Y. Kim[a]**

[a]Department of Mechanical and Materials Engineering, Queen's University

[b]Konkuk Aerospace Design-Airworthiness Research Institute, Konkuk University

[c]Korea Institute of Carbon Convergence Technology

E-mail: kimiy@queensu.ca

## Abstract

Increased urban expansion in recent years has uncovered an inefficiency in mid-range travel. Urban Air Mobility (UAM) aims to address this gap using hybrid and full-electric Personal Air Vehicles (PAVs) as a source of accessible, on-demand transportation. To achieve success with PAVs, reduction of mass is imperative due to the current battery capacity constraints. Many VTOL (Vertical Takeoff and Landing) PAV designs use multi-propulsor configurations which fix propulsor assemblies away from the main airframe using cantilevered boom structures. Booms must be lightweight to ensure aircraft efficiency but meet the structural requirements. This can be achieved using advanced materials such as Carbon Fibre Reinforced Polymers (CFRPs) paired with advanced design tools such as composite laminate optimization. Presently, existing literature in UAM design is focused on conceptual design optimization with high-level structural considerations for only conventional materials, which leaves significant weight savings unrealized. This work addresses this knowledge gap by presenting a detailed structural optimization methodology for PAV propulsor boom design applied to a PAV concept created in collaboration with Queen's University, Konkuk University, and KCTECH. A comparison between the proposed design and a conventional design, with aluminum and standard optimization methodologies, shows a mass reduction of 74.6% using the advanced optimization approach.

**Keywords –**

**Laminate optimization, Personal Air Vehicles, Urban Air Mobility, Shape optimization.**

## 1 Introduction

Rapid urbanization recently has contributed to an increasing need for on-demand transportation over mid-range distances (80-800km), which is inefficient using traditional means of transport. Urban Air Mobility (UAM) is a disruptive concept that aims to address this gap using hybrid and full-electric Personal Air Vehicles (PAVs) as a source of accessible, on-demand transportation. Given energy density constraints associated with current battery technology, the reduction of structural mass in PAVs is imperative to achieving success in UAM design. Until recently, several limitations prohibited significant development of UAM, however, timely technological advances and depleting resource availability make now the right time to explore these transformative aircraft technologies [1]. Hundreds of start-ups and established aerospace companies are currently developing PAV concepts, with almost all using battery or hybrid-electric power sources. These PAV designs commonly feature multi-propulsor configurations which use booms to fix propulsor assemblies away from the main airframe. Boom structures must be strong and stiff to withstand large cantilevered thrust loads, yet lightweight to ensure aircraft efficiency and overcome mass constraints imposed by electric propulsion. Computational design optimization techniques and advanced composite materials, such as Carbon Fibre Reinforced Polymers (CFRP), are both promising avenues for meeting this requirement.

Recent research has incorporated advanced composites into computational design optimization and has shown to be effective in further reducing mass. Laminate optimization is a design technique used to determine an optimum distribution of composite plies in manufacturable laminates within a given design domain to maximize a performance measure subject to design constraints. Shrivastava et al. [2] proposed a multi-objective, multi-laminate design optimization methodology for composite structures using genetic algorithms. This approach was applied to the design of a wing torsion box showing a 54% reduction in mass compared to an aluminum design. Kupchanko et al. [3] applied a topology and CFRP laminate optimization approach in Altair Optistruct to reduce the compliance of an aircraft seat by 8% relative to an aluminum 2024 design of the same mass.

Recent publications in PAV conceptual design have shown performance improvements through the

implementation of conceptual design optimization methodologies. Clarke et al. [4] proposed several potential multidisciplinary conceptual design optimization approaches for minimising the maximum takeoff weight (MTOW), mission time, and energy consumption. Optimization for mass yielded a reduction in MTOW (9.2%), battery energy consumption reductions (10.8%), and total mission time (3.3%). Hendricks et al. [5] presented a multidisciplinary optimization methodology for PAV design with the objective of reducing initial fuel mass. This was applied by changing conceptual design variables such as propeller speed, wingspan, wing twist, and cruise altitude subject to structural, propulsion, and trajectory constraints. Optimization yielded a fuel consumption reduction of 15.5%. Presently, existing literature on PAV design is focused on conceptual design optimization with high-level structural considerations. By focusing on high-level conceptual design parameters and considering only conventional structural materials, these approaches leave weight savings unrealized.

The objective of this work is to present a structural optimization approach for detailed PAV boom design and to apply the method on a concept shown in Figure 1 - created in collaboration with Queen's University, Konkuk University, and KCTECH. Two optimization methodologies will be applied to a conventional aluminum design and an advanced CFRP design. The conventional design optimization methodology will use simultaneous gauge thickness and shape optimization to minimize mass subject to stress and displacement constraints. The advanced design optimization methodology will use simultaneous laminate and shape optimization to minimize mass subject to composite failure and displacement constraints. The designs will be compared in terms of mass, stiffness, and strength to demonstrate the applicability of advanced design optimization methodologies and the benefits of CFRP to UAM.

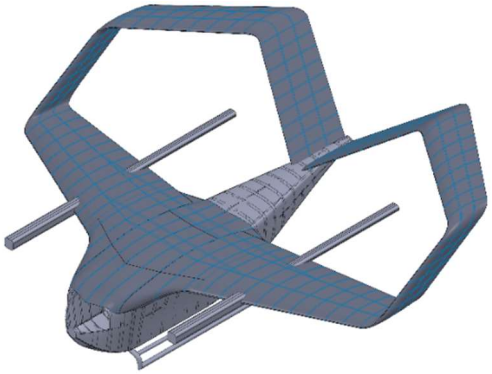

**Figure 1: PAV concept developed in collaboration with KCTECH and Konkuk University.**

## 2 Methodology

The Altair Hyperworks software suite is used for the structural optimization process, where Hypermesh is used for model pre-processing, and Optistruct is used as the Finite Element (FE) solver.

### 2.1 Gauge Thickness Optimization

Gauge optimization is a form of size optimization in which the thickness, or gauge, of a component is optimized. This type of optimization is confined to 2D elements (shells) and the design variables considered are the properties (thickness) associated with each component as defined in the Finite Element (FE) model. This method is preferable in comparison to free size optimization when applied to aluminum as it results in uniform optimized thickness at the component level, as opposed to the individual element level, which drastically reduces the complexity of the design interpretation required for manufacturability.

### 2.2 Laminate Optimization

Composite materials generally consist of a strong, stiff, but brittle fiber (ex. carbon) material, which is held within a matrix of a weaker/compliant but more ductile polymer (resin). This composition allows for the composite material to have strong/stiff material properties of the fiber while reducing brittleness from the addition of the polymer. In a unidirectional configuration, fibers are laid up along one direction, giving the composite superior strength/stiffness in that direction. Bidirectional configurations use woven fibers aligned along two perpendicular directions, giving superior strength/stiffness in both directions. The directionality of composite material stiffness is modelled in Finite Element Analysis (FEA) by adding an auxiliary material coordinate system, the principal directions of which model the direction of the fibers. A difference between the material coordinate system relative to the element coordinate system models a layup with a non-zero-degree ply orientation to change the directional strength properties.

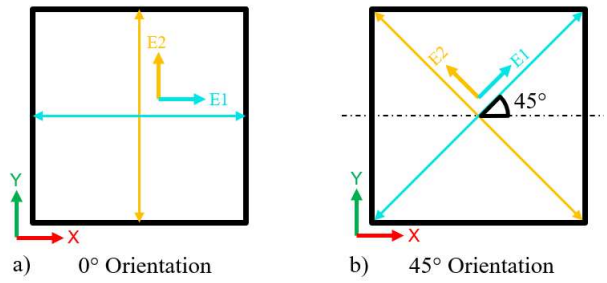


**Figure 2: Representation of two possible ply orientations relative to the element coordinate system.**

In a standard 0-degree orientation ply, the principal axes of the material coordinate system are directly in-line with the element coordinate system. Figure 2a shows a 0-degree orientation where E1 and E2 (the composite principal axes) in the material coordinate system are parallel to X and Y in the element coordinate system, respectively. Figure 2b shows a 45-degree orientation where E1 and E2 are not directly aligned with the element coordinate system. The 45-degree orientation gives the element more stiffness in off-axis directions, which can be useful when loads are not applied parallel or perpendicular to the element axes. Laminate optimization leverages this directionality in the optimization process, strategically adding thickness in off-angle orientation plies to assist with off-angle loading.

Laminate optimization is performed using a three-stage approach, consisting of a free-size (thickness) optimization, discrete size optimization, and a ply stacking sequence optimization.

**Free Size Optimization (FSO)** allows for the most design freedom of any thickness optimization methodology, as the thicknesses of multiple ply orientations within each element are continuously variable throughout the entire design domain. After the free size optimization, a set of ply bundles are determined, which correspond to the thickness requirements for each orientation in each element (in this case, 0 degrees, 45 degrees, -45 degrees, and 90 degrees). The ply bundles consist of a user defined number of ply shapes (default = 4) which have variable shapes and thicknesses to best approximate the free-size result for that given orientation. Figure 3 shows a simplified example of how the free-size result for a single orientation is translated to ply bundles. A 4-element square with a variable thickness is broken into 4 shapes – shape 1 being the "base" layer for all elements (ie. it represents the minimum thickness for all elements for this orientation), and subsequent shapes, with some elements removed, being stacked on top of each other. The maximum thickness of the element(s) is where all 4 ply shapes "intersect" and the minimum at the element(s) where only 1 ply shape is present. This method does not provide a perfect representation of the FSO result when scaled up to the size of the boom problem, as 4 ply shapes do not provide infinite "resolution" for the distribution of thicknesses.

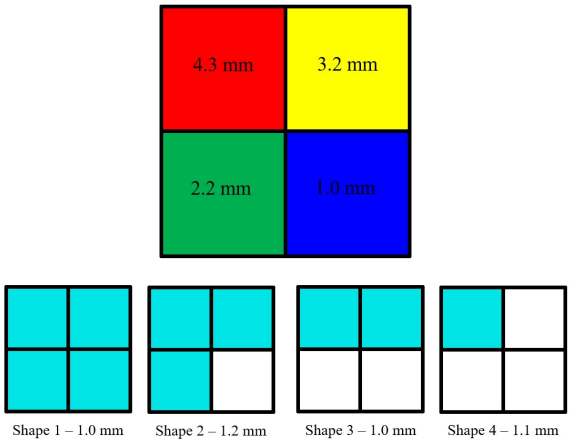


**Figure 3: Simplified example of the Free-Size to ply-bundle translation.**

**Discrete Size Optimization (DSO)** is used to create manufacturable laminates by breaking up each of the ply shapes from the FSO stage into multiples of the manufacturable ply thickness (user defined). The discretization does not perfectly replicate the requested thicknesses from FSO, and therefore a size optimization of each ply bundle with discrete thickness intervals (ply thickness) is performed to re-work the design and improve performance of the design objective.

**Ply Stacking Sequence Optimization (PSSO)** takes the DSO result and performs optimization to re-order the sequence of plies within the laminate, such that it abides by the manufacturability requirements for laminates. The requirements include specifying symmetrical placements of specific ply orientations around the centre of the laminate, as well as a maximum number of successive layers of the same ply orientation. Figure 4 is a simplified example of the PSSO process applied to a fictional laminate with 4 orientations and 2 plies-per-orientation. The manufacturability requirements for this PSSO enforce symmetrical 45.0 and -45.0 degree plies and a maximum successive ply shape layer limit of 1.

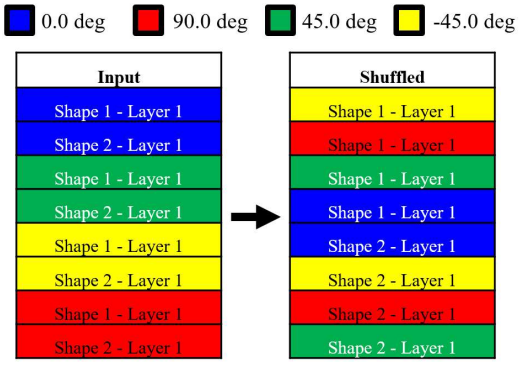


**Figure 4: Simplified example of the PSSO stage.**

### 2.3 Shape Optimization

Shape optimization is a form of optimization which varies the position of geometric features (often FE nodes) to improve a given objective response. Nodes are specified to move along selected paths to change the shape of the design. Shape optimization is performed in conjunction with Laminate Optimization in the CFRP case, and with Gauge Optimization in the aluminum case. Simultaneously performing shape and thickness optimization adds additional design freedom to further optimize the load paths generated with laminate and gauge optimization.

## 3 Optimization Setup

### 3.1 Materials

The material used for the CFRP design is a woven fabric prepreg developed by KCTECH [6]. The aluminum alloy chosen is a standard aerospace grade sheet material (2024-T4). Properties for these two materials can be found in Table 1.

**Table 1: Table of material properties for the two main construction materials.**

| Material Property | Aluminum 2024 – T4 [7] | KCTECH Woven Fabric Prepreg [6] |
|---|---|---|
| $E_{11}, E_{22}$ [GPa] | 73.00 | 69.38 |
| Tensile Strength, [MPa] | 325.0 | 1115 |
| Compressive Strength [MPa] | 325.0 | 800.0 |
| Shear Strength [MPa] | 325.0 | 59.32 |
| Density [g/cm$^3$] | 2.780 | 1.500 |

The Tsai-Wu composite failure criterion is chosen to predict failure of the woven fabric prepreg material, and the Von-Mises failure criterion is chosen to predict material failure for the aluminum design. The Tsai-Wu failure theory uses multiple strength parameters to predict failure based on directional stresses. Failure is predicted when the composite failure index reaches 1, which is described mathematically by the following general equation:

$$F_i\sigma_i + F_{ij}\sigma_i\sigma_j \le 1 \qquad \text{for } i, j = 1,\ldots,6 \qquad (1)$$

where $F$ is the tensor of determined material strength parameters and $\sigma$ is the vector of measured stresses. For the woven fabric prepreg material used in this study, equation (1) can be written in terms of the strength input variables (listed in Table 1) as follows:

$$\left(\frac{1}{X_T}-\frac{1}{X_C}\right)\sigma_1+\left(\frac{1}{Y_T}-\frac{1}{Y_C}\right)\sigma_2+\frac{\sigma_1^2}{X_TX_C}+\frac{\sigma_2^2}{Y_TY_C}+\frac{\sigma_6^2}{S^2}+2S\sigma_1\sigma_2 \le 1 \qquad (2)$$

where $X_T, Y_T$ are the tensile strengths in the 1st and 2nd principal directions respectively, $X_C, Y_C$ are the compressive strengths in the 1st and 2nd principal directions respectively, $S$ is the shear strength (in plane), $\sigma_1, \sigma_2$ are the stresses in the 1st and 2nd principal directions respectively, and $\sigma_6$ is the shear stress in plane.

### 3.2 FEA Models

The initial design for the boom is a simple hollow square beam structure with mounting holes for fastening to the wings through the ribs. Propulsors, which attach to the end of the booms, are represented by rigid elements that fix relative displacement between nodes at the mounting points (see Figure 5).

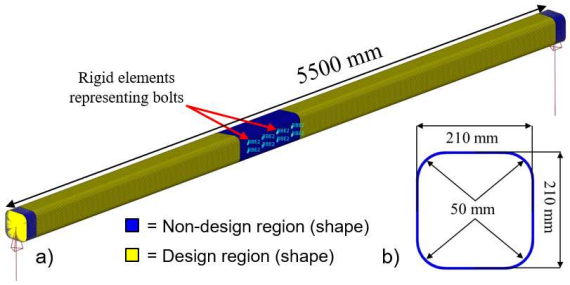


**Figure 5: a) Isometric view and b) front view of the boom FEA model with dimensions. The design regions for shape optimization are shown – all shell elements are designable for thickness optimization.**

Four load cases are applied to the boom, shown in Table 2. Load case 1 represents a maximum-power ascent, Load case 2 represents a rear propulsor failure with maximum thrust, Load case 3 represents a front propulsor failure with maximum thrust, and Load case 4 represents a forward flight state at maximum forward thrust. These load cases were defined during the conceptual design phase of the PAV concept developed in collaboration between KCTECH, Konkuk University, and Queen's University.

**Table 2: Set of forces applied to the propulsor attachment points for the 4 loading cases.**

| Load Case | Front Rotor Load (N) | | | Rear Rotor Load (N) | | |
|---|---|---|---|---|---|---|
| | X | Y | Z | X | Y | Z |
| 1 | - | 5,518 | - | - | 5,518 | - |
| 2 | - | 5,518 | - | - | - | - |

| | | | | | | |
|---|---|---|---|---|---|---|
| **3** | - | - | - | - | 5,518 | - |
| **4** | -685 | - | - | - | - | - |

### 3.3 Aluminum Gauge Optimization

Gauge optimization is applied to the aluminum boom design, with the objective of minimizing the overall mass of the structure while maintaining a maximum tip displacement of 100mm and a safety factor against yielding of 1.5. The boom is broken into 48 panels, which act as the gauge optimization design variables. The baseline design has an initial thickness for each panel of 5mm.

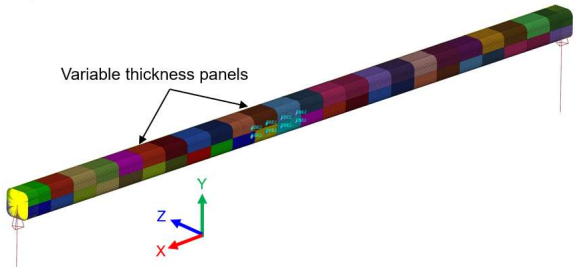


**Figure 6: Isometric view of the aluminum thickness optimization setup, where the different colours represent panels acting as gauge design variables.**

The shape optimization conducted in this paper is performed using 36 morphing volumes which allow the cross section of the boom to shrink to 50% and grow to 125% of the original dimensions uniformly as to ensure manufacturable designs (see Figure 7).

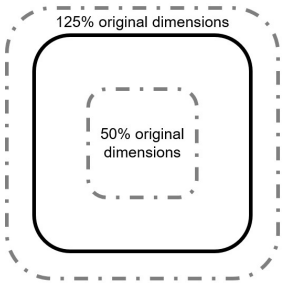


**Figure 7: Diagram showing the range of shape changes possible in the shape optimization phase for aluminum and CFRP designs.**

The gauge optimization is performed with the following problem statement:

$$\text{Minimize: } \text{mass}\left(\underset{\sim}{t}, \underset{\sim}{\Delta}\right) \quad (3)$$

Subject to: $\sigma_i \le 216.6\overline{6}$MPa i = 1,2,3,4 load cases

$u_{tip,i} \le 100$mm

$t_j \in \{1.016, 1.270, 1.600, 1.803, 2.032,$
$2.286, 3.175, 4.064, 4.826, 6.350\}$ mm

j = 1,…,48 designable panels

$27.5 \le \Delta_l \le 68.75$ mm

l = 1,…,36 morphable volumes

where $\sigma$ stress for all elements [MPa], $\underset{\sim}{t}$ is a vector of panel thicknesses [mm] $u_{tip}$ is the displacement at the tip of the boom [mm], and $\underset{\sim}{\Delta}$ is a vector of side lengths for shape optimization [mm].

### 3.4 CFRP Laminate Optimization

The 3-stage laminate optimization approach is applied to the CFRP boom design. The objective of the optimization is to minimize the overall mass of the structure while maintaining a maximum tip displacement of 100mm and a safety factor against composite failure of 1.5. Shape optimization applied to the CFRP design is performed using the same optimization setup as with the aluminum gauge optimization. The initial design is modelled with a 4-orientation laminate with each orientation being 1mm thick (4mm total thickness for all elements). The FSO and shape optimization stage is performed with the following problem statement:

$$\text{Minimize: } \text{mass}\left(\underset{\sim}{t}, \underset{\sim}{\theta}, \underset{\sim}{\Delta}\right) \quad (4)$$

Subject to: $CFI_i \le 0.44\overline{4}$ i = 1,2,3,4 load cases

$u_{tip,i} \le 100$mm

$0.6\text{mm} \le t_j \le 4.8\text{mm}$

j = 1,…,41815 designable elements

$\theta_k^j \in \{0°, 45°, -45°, 90°\}$

k = 1,2,3,4 orientations for a given element j

$27.5 \le \Delta_l \le 68.75$

l = 1,…,36 morphing volumes

where $CFI$ is the Tsai-Wu composite failure index for all elements [], $\underset{\sim}{t}$ is a vector of element thicknesses [mm], $\underset{\sim}{\theta}$ is a vector of ply orientation angles [°], and $\underset{\sim}{\Delta}$ is a vector of side lengths for shape optimization [mm].

The DSO stage is performed to produce a manufacturable design, in this case with 0.2mm thick plies and a minimum laminate thickness of 0.6mm. To setup the optimization, the resultant ply shapes from the free-size optimization output are cleaned of "stray" elements without connections. Additionally, due to the inclusion of shape optimization, the ply shapes (which are created for the original mesh) must be projected to the mesh of the optimized shape. The DSO problem statement is as follows:

$$\text{Minimize: } \text{mass}\left(\underset{\sim}{t}\right) \quad (5)$$

Subject to: $CFI_i \le 0.44\overline{4}$ i = 1,2,3,4 load cases

$u_{tip,i} \le 100$mm

$$0.0\text{mm} \le t_j \le 4.8\text{mm},\ \Delta t_{ply} = 0.2\text{mm}$$
$$\text{j} = 1,\ldots,4 \text{ designable ply bundles}$$
$$0.6\text{mm} \le t_{lam} \le 4.8\text{mm},\ \Delta t_{lam} = 0.2\text{mm}$$

where $\underset{\sim}{t}$ is a vector of ply bundle thicknesses [mm], $\Delta t_{ply}$ is the discrete interval between ply bundle thicknesses [mm], $t_{lam}$ is the total thickness of the laminate [mm], and $\Delta t_{lam}$ is the discrete interval between laminate thicknesses [mm].

The PSSO stage does not use a mass minimization objective, as no plies are added/removed. The objective for this stage is to meet all laminate manufacturability requirements and previous design requirements. The manufacturability requirements specify that -45 degree and 45-degree plies are symmetrical about the middle of the laminate, and that the maximum successive plies of the same shape is 2.

# 4 Optimization Results

## 4.1 Aluminum Gauge Optimization

Figure 8 shows a contour plot of the gauge optimization result, which has a total mass of 30.60kg – a reduction of 69.0% relative to the baseline design with a 5mm thickness. The optimized shape shows a significant cross sectional area reduction near to the propulsor mounts, with a gradual transition to the non-designable centre section where the model is constrained. Table 3 shows that the optimized design meets all design constraints.

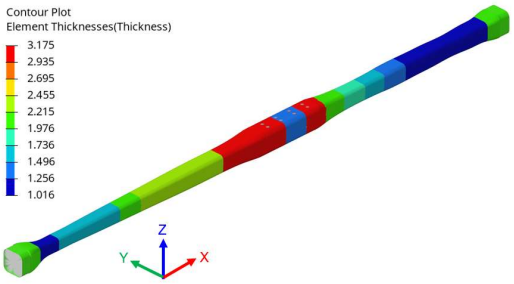


**Figure 8: Contour plot and associated scale (mm) for the thicknesses of each component of the optimized aluminum result.**

**Table 3: Comparison between the baseline and gauge optimized aluminum result in terms of structural performance.**

| Design | Mass [kg] | Max. tip disp. [mm] | Stress [MPa] | Safety Factor [] |
|---|---|---|---|---|
| **Baseline** | 98.82 | 24.27 | 147.5 | 2.203 |
| **Gauge** | 30.60 | 100.0 | 216.7 | 1.500 |

## 4.2 CFRP Laminate Optimization

Figure 9 shows a contour plot of the FSO and shape optimization result, which has a total mass of 5.88kg – a reduction of 78.0% relative to the baseline design. The resulting ply bundles from this optimization are non-manufacturable, as their thicknesses are not bound by the discrete 0.2mm ply thickness constraint. Figure 10 shows an example of the four ply shapes for one of the ply bundles (0-degree orientation). The thickness of these plies are made manufacturable and subsequently re-optimized in the DSO stage. The shape optimization produces a gentle taper from the middle non-design space to the ends where the propulsor non-design space begins. This reduction in cross sectional area coincides with where the design has reduced material thicknesses – showing that the shape is reducing volume (and therefore sacrificing stiffness) strategically where the maximum stiffness is not required.

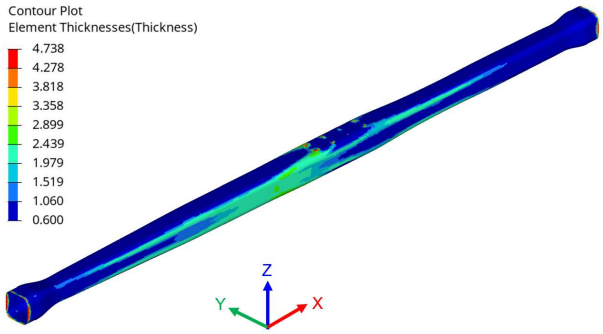


**Figure 9: Contour plot and associated scale [mm] of the free-size optimization result for the CFRP laminate optimization.**

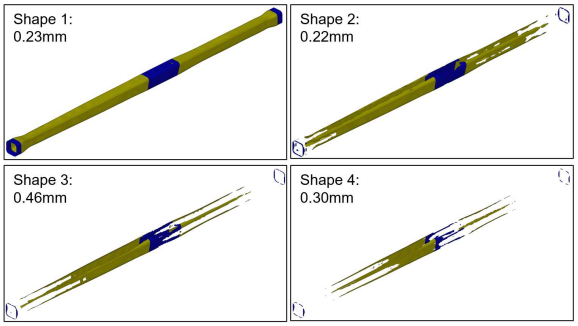


**Figure 10: Resulting ply shapes and thicknesses for the 0-degree ply bundle.**

The subsequent DSO stage resulted in a mass increase of 32%, to 7.764kg. This is expected given that the design is restricted to manufacturable ply thicknesses with increments of 0.2mm rather than them being continuously variable. Figure 11 shows the total

thickness of all elements, which is the sum of individual ply shape layers within each bundle for each orientation. A comparison of the FSO stage ply thicknesses and the DSO ply shape layers is shown in Table 4.

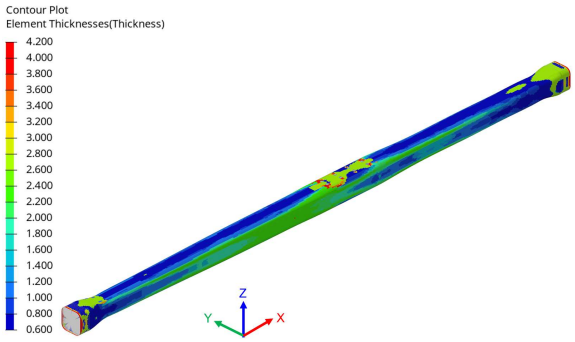


**Figure 11: Contour plot and associated scale [mm] of the discrete-size optimization result for the CFRP laminate optimization.**

**Table 4: Thicknesses of the resulting ply shapes for each orientation from the free-size optimization result, and the resulting ply layers from the discrete-sizing optimization result (each 0.2mm thick).**

| Orientation [deg.] | Ply Shape | Thickness from FSO + Shape opt. [mm] | Ply Shape Layers from DSO [] |
|---|---|---|---|
| 0 | 1 | 0.23 | 1 Layer |
| 0 | 2 | 0.22 | 1 Layer |
| 0 | 3 | 0.46 | 2 Layers |
| 0 | 4 | 0.30 | 1 Layer |
| 45 | 1 | 0.03 | 1 Layer |
| 45 | 2 | 0.05 | 0 Layers |
| 45 | 3 | 0.07 | 0 Layers |
| 45 | 4 | 1.06 | 4 Layers |
| -45 | 1 | 0.03 | 0 Layers |
| -45 | 2 | 0.05 | 0 Layers |
| -45 | 3 | 0.07 | 0 Layers |
| -45 | 4 | 1.06 | 6 Layers |
| 90 | 1 | 0.22 | 1 Layer |
| 90 | 2 | 0.23 | 1 Layer |
| 90 | 3 | 0.44 | 2 Layers |
| 90 | 4 | 0.31 | 1 Layers |

The PSSO stage does not alter the mass of the design due to the same plies and thicknesses being present in the initial and optimal designs. The PSSO in this case, shown in Table 5, results in an increase of displacement without change to the CFI, which is possible due to the imposition of additional constraints on the laminate design.

**Table 5: Table of the laminate ply stacking sequence before and after the ply stacking sequence optimization stage.**

0.0 deg  90.0 deg  45.0 deg  -45.0 deg

| Discrete Sizing Optimization Result | Ply Stacking Sequence Optimization Result |
|---|---|
| Shape 1 - Layer 1 | Shape 1 - Layer 1 |
| Shape 2 - Layer 1 | Shape 4 - Layer 1 |
| Shape 3 - Layer 1 | Shape 1 - Layer 1 |
| Shape 3 - Layer 2 | Shape 1 - Layer 1 |
| Shape 4 - Layer 1 | Shape 4 - Layer 1 |
| Shape 1 – Layer 1 | Shape 4 - Layer 2 |
| Shape 4 - Layer 1 | Shape 2 - Layer 1 |
| Shape 4 - Layer 2 | Shape 2 - Layer 1 |
| Shape 4 - Layer 3 | Shape 4 - Layer 2 |
| Shape 4 - Layer 4 | Shape 4 - Layer 3 |
| Shape 4 - Layer 1 | Shape 3 - Layer 1 |
| Shape 4 - Layer 2 | Shape 3 - Layer 1 |
| Shape 4 - Layer 3 | Shape 4 - Layer 3 |
| Shape 4 - Layer 4 | Shape 4 - Layer 4 |
| Shape 4 - Layer 5 | Shape 3 - Layer 2 |
| Shape 4 - Layer 6 | Shape 3 - Layer 2 |
| Shape 1 - Layer 1 | Shape 4 - Layer 4 |
| Shape 2 - Layer 1 | Shape 4 - Layer 5 |
| Shape 3 - Layer 1 | Shape 4 - Layer 1 |
| Shape 3 - Layer 2 | Shape 4 - Layer 1 |
| Shape 4 - Layer 1 | Shape 4 - Layer 6 |

A summary of the design evolution through the 3 stages of the laminate optimization process is shown in Table 6.

**Table 6: Comparison of the mass results for 3 stages of the CFRP laminate optimization in terms of structural performance.**

| Design | Mass [kg] | Max. tip disp. [mm] | CFI [] | Safety Factor [] |
|---|---|---|---|---|
| **Baseline** | 26.79 | 38.29 | 0.265 | 1.943 |
| **FSO + Shape** | 5.884 | 100.5 | 0.464 | 1.468 |
| **DSO** | 7.764 | 95.11 | 0.428 | 1.529 |
| **SSO** | 7.764 | 95.87 | 0.428 | 1.529 |

### 4.3 Results Comparison

It can be seen from Table 7 that the use of CFRP gives significant performance benefits relative to the Aluminum design. The mass of the optimized CFRP design is 74.6% less than that of the optimized aluminum design while meeting all design requirements. This superior design is due to the high material performance and the advanced optimization techniques possible for CFRP. The properties of the CFRP can be directionally customized to better suit the applied loads.

**Table 7: Comparison of the performance of the two optimized designs.**

| Design | Mass [kg] | Max. tip disp. [mm] | Safety Factor [] |
|---|---|---|---|
| **Aluminum – Gauge & Shape Opt.** | 30.60 | 100.0 | 1.500 |
| **CFRP – Laminate & Shape Opt.** | 7.764 (-75%) | 95.87 (-4%) | 1.529 (+2%) |

To assess the impact of the laminate optimization technique, the CFRP design was re-optimized using only shape and gauge optimization. This resulted in an optimized mass of 8.143kg – 4.88% heavier than the laminate optimized result, but still 73.4% lighter than the aluminum design.

## 5. Conclusions

This investigation into a detailed laminate optimization methodology and its application to a PAV boom design has shown the effectiveness of using advanced optimization techniques for composite materials such as CFRP. Additionally, it was shown that the inclusion of simultaneous shape optimization can further reduce mass when advanced optimization methodologies are used. Future work includes adapting this methodology to more systems within the PAV design to provide a full design optimization methodology for UAM. Additionally, future work would address additional advanced load cases such as time-dependent thrust and responses from the rotor vibrations.

## References

[1] W. Johnson and C. Silva, "Observations from Exploration of VTOL Urban Air Mobility Designs," NASA, 2018.

[2] S. Shrisvastava, P. M. Mohite, T. Yadav and A. Malaguadanavar, "Multi-objective Multi-Laminate Design and Optimization of a Carbon Fibre Composite Wing Torsion Box Using Evolutionary Algorithm," *Composite Structures,* vol. 185, pp. 132-147, 2018.

[3] L. Kupchanko, S. W. K. Roper, H. Lee, M. Huh and I. Y. Kim, "A Comparison of Lightweight Design Concepts of a Passenger Aircraft Seat Using Topology and CFRP Laminate Optimization," in *CSME Congress*, Charlottetown, 2020.

[4] M. Clarke, J. Smart, E. Botero, W. Maier and J. J. Alonso, "Strategies for Posing a Well-Defined Problem for Urban Air Mobility Vehicles," in *AIAA SciTech Forum*, San Diego, 2019.

[5] E. S. Hendricks, R. D. Falck, J. S. Gray, E. D. Aretskin-Hariton, D. J. Ingraham, J. W. Chapman, S. L. Schnulo, J. C. Chin, J. P. Jasa and J. D. Bergeson, "Multidisciplinary Optimization of a Turboelectric Tiltwing Urban Air Mobility Aircraft," in *AIAA Aviation Forum*, Dallas, 2019.

[6] KCTECH, "Woven Fabric Prepreg & LFPS," KCTECH, Jeonju, 2020.

[7] ASM International, "Properties and Selection: Nonferrous Alloys and Special-Purpose Materials," in *Metals Handbook, Vol. 2*, ASM International, 1990.